To test the generality of these results, the photochemistry of the trisubstituted dibenzobarrelenes **4b** (E = CO_2Me; R_1 = Me; R_2 = H) and **4c** (E = CO_2Me; R_1 = Ph; R_2 = H) was investigated. In each case, both in the solid state and in solution, the COT formed was that derived from Grob fragmentation rather than $2\pi + 2\pi$ photocycloaddition. In neither case, however, was a photoproduct analogous to diester **5** isolated. The structures of both COTs were determined by X-ray crystallography.[3] This corrects an earlier publication from our group in which the COT from **4b** was assumed to have the $2\pi + 2\pi$ derived structure.[7,8] One might ask whether *all* dibenzobarrelenes give Grob fragmentation COTs. They do not. X-ray data indicate that the COT from 9-isopropyl 11-methyl 9,10-dihydro-9,10-ethenoanthracene-9,11-dicarboxylate is of the $2\pi + 2\pi$ type.[9]

The origin of biradical **8** presents an interesting mechanistic problem. Most likely of singlet multiplicity (since neither of the photoproducts thought to be derived from it are formed in the triplet-sensitized reaction), its formation involves, at least formally, a type of "tri-π-methane" interaction of both aromatic rings with the aliphatic double bond.[10] The simplest mechanism among several that will be discussed in a full paper involves direct (although probably not concerted[11]) rearrangement of **4a** to **8** (mechanistic arrows, Scheme II). The reluctance of **4a** to engage in $2\pi + 2\pi$ photocycloaddition can be attributed reasonably to steric factors. This, coupled with the additional stability afforded biradical **8** by the methyl substituents, plausibly rationalizes the unexpected singlet-state behavior of **4a**; similar arguments apply in the case of dibenzobarrelene derivatives **4b** and **4c**.[12] Current research is concerned with further elaborating the structural and environmental factors responsible for the novel photoreactivity.

Acknowledgment is made to the donors of the Petroleum Research Fund, administered by the American Chemical Society, for partial support of this research. Financial support by the Natural Sciences and Engineering Research Council of Canada is also gratefully acknowledged.

Registry No. 4a, 1100-93-2; **4b**, 58802-07-6; **4c**, 77452-72-3; **5**, 125903-02-8; **6**, 125903-03-9; **7**, 125903-01-7.

(6) It might at first sight seem that COT **6** could be formed through photoisomerization of an initially formed $2\pi + 2\pi$ derived COT. For example, Stiles and Burckhardt (Stiles, M.; Burckhardt, U. *J. Am. Chem. Soc.* **1964**, *86*, 3396) and Salisbury (Salisbury, L. E. *J. Org. Chem.* **1978**, *43*, 4987) have shown that 5,6-disubstituted COTs rearrange to their 5,11 isomers via "crossed" [2 + 2] photocycloaddition followed by thermal ring opening in the opposite sense. This mechanism, when applied to the hypothetical $2\pi + 2\pi$ COT from **4a**, returns the starting material. A second concern that can be dismissed with a little thought is the possibility that di-π-methane photoproduct **7** could be confused with the hypothetical product resulting from coupling of biradical **8**. The ^1H NMR spectrum of **7**, however, which shows two nonequivalent methyl ester resonances at δ 3.76 and 3.88 and two additional nonequivalent methyl singlets at δ 1.90 and 1.98, clearly rules out this possibility. As added evidence, crystallography shows that the di-π-methane photoproduct from dibenzobarrelene derivative **4c** has the expected structure: Trotter, J.; Pokkuluri, P. R., unpublished results.

(7) Pokkuluri, P. R.; Scheffer, J. R.; Trotter, J. *Tetrahedron Lett.* **1989**, *30*, 1601.

(8) Other workers have assigned $2\pi + 2\pi$ structures to COTs derived from bridgehead-substituted dibenzobarrelene derivatives. See, for example, ref 2b. See also: Kumar, C. V.; Murty, B. A. R. C.; Lahiri, S.; Chackachery, E.; Scaiano, J. C.; George, M. V. *J. Org. Chem.* **1984**, *49*, 4923. Pratapan, S.; Ashok, K.; Cyr, D. R.; Das, P. K.; George, M. V. *J. Org. Chem.* **1987**, *52*, 5512.

(9) Pokkuluri, P. R.; Scheffer, J. R.; Trotter, J. Unpublished results.

(10) The "tri-π-methane" terminology is borrowed from Zimmerman, who coined it some time ago and used it recently in describing the unusual solid-state photorearrangement of an aliphatic trivinylmethane derivative to a substituted vinylcyclopentene. See: Zimmerman, H. E.; Zuraw, M. J. *J. Am. Chem. Soc.* **1989**, *111*, 7974.

(11) In considering possible mechanisms for the di-π-methane photorearrangement of barrelene, Zimmerman et al. (Zimmerman, H. E.; Binkley, R. W.; Givens, R. S.; Sherwin, M. A. *J. Am. Chem. Soc.* **1967**, *89*, 3932) concluded, on the basis of extended Hückel calculations, that concerted double bridging has a relatively high activation barrier compared to the corresponding stepwise process.

(12) The reason why **4a** affords the diester migration product **5** when photolyzed in the solid state, whereas **4b** and **4c** do not, is not clear at the present time. We tentatively ascribe this to crystal packing effects that are unique to **4a**.

In Situ Scanning Tunneling Microscopy of Adsorbates on Electrode Surfaces: Images of the ($\sqrt{3}\times\sqrt{3}$)R30°-Iodine Adlattice on Platinum(111)

Shueh-Lin Yau, Carissima M. Vitus, and Bruce C. Schardt*

Department of Chemistry, Purdue Univeristy
West Lafayette, Indiana 47907

Received November 30, 1989

In the study of electrified interfaces, it is extremely difficult to acquire information concerning the detailed structure of the interfacial region. Two promising methods for in situ characterization of electrode surfaces are scanning tunneling microscopy (STM)[1] and atomic force microscopy (AFM).[1,2] Application of STM to the study of metal surfaces in situ has been limited to the observation of gross-scale (1 nm to 1 μm) morphological features as illustrated by several studies of the effect of surface pretreatments on the roughness of platinum electrodes.[3,4] Other studies of this type have looked at electrodeposition processes[5-10] and stainless steel.[11] Improved resolution leading to the observation of monoatomic steps has been achieved by only a few researchers using either single crystals or evaporated films.[12,13]

In this communication, we report further improvement in the resolution attainable with an STM operating in situ. We have imaged the ($\sqrt{3}\times\sqrt{3}$)R30°-I adlattice on a Pt(111) single crystal in aqueous 0.1 M $HClO_4$. This suggests that STM has a bright future as a tool for studying fundamental processes at electrode surfaces. We have also managed to find conditions that allowed imaging the Pt(111) substrate lattice in ambient laboratory air. The Pt(111) substrate lattice image aids in interpretation of the in situ images.

Iodine dosing of a platinum(111) surface in ultrahigh vacuum (UHV) produces two ordered adlattices.[14] At a fractional surface coverage of 0.33, the iodine orders into a ($\sqrt{3}\times\sqrt{3}$)R30° lattice with one iodine atom per surface unit cell. At a fractional coverage of 0.43, the iodine orders into a ($\sqrt{7}\times\sqrt{7}$)R19.1° unit cell containing three iodine atoms. The ($\sqrt{7}\times\sqrt{7}$)R19.1° phase can be prepared by a convenient gas-phase dosing procedure that does not require the use of UHV.[15,16] The procedure involves annealing the single-crystal surface in a hydrogen flame followed by cooling in a glass dosing cell containing iodine crystals and being purged with N_2. In previous research, we were able to use STM to image the ($\sqrt{7}\times\sqrt{7}$)R19.1° phase of iodine in the ambient laboratory atmosphere.[17]

(1) Binnig, G.; Rohrer, H.; Gerber, C.; Weibel, E. *Appl. Phys. Lett.* **1981**, *40*, 178.
(2) Binnig, G.; Quate, C. F.; Gerber, C. *Phys. Rev. Lett.* **1986**, *56*, 930-933.
(3) Fan, F.-R. F.; Bard, A. J. *Anal. Chem.* **1988**, *60*, 751-758.
(4) Arvia, A. J.; Salvarezza, R. C.; Triaca, T. *Electrochim. Acta* **1989**, *34*, 1057-1071.
(5) Van Der Eerden, J. P.; Mickers, M. A. H.; Gerritsen, J. W.; Hottenhuis, M. H. J. *Electrochim. Acta* **1989**, *34*, 1141-1145.
(6) Uosaki, K.; Kita, H. *J. Electroanal. Chem.* **1989**, *259*, 301-308.
(7) Hottenhuis, M. H. J.; Mickers, M. A. H.; Gerritsen, J. W.; Van Der Eerden, J. P. *Surf. Sci.* **1988**, *206*, 259-278.
(8) Armstrong, M. J.; Muller, R. H. *J. Electrochem. Soc.* **1989**, *136*, 584.
(9) Green, M. P.; Hanson, K. J.; Scherson, D. A.; Xing, X.; Richter, M.; Ross, P. N.; Carr, R.; Lindau, I. *J. Phys. Chem.* **1989**, *93*(6), 2181-2184.
(10) Cristoph, R.; Siegenthaler, H.; Rohrer, H.; Wiese, H. *Electrochim. Acta* **1989**, *34*, 1011-1022.
(11) Fan, F.-R. F.; Bard, A. J. *J. Electrochem. Soc.* **1989**, *136*, 166-170.
(12) Wiechers, J.; Twomey, T.; Kolb, D. M.; Behm, R. J. *J. Electroanal. Chem.* **1988**, *248*, 451-460.
(13) Trevor, D.; Chidsey, C. E. D.; Loiacono, D. N. *Phys. Rev. Lett.* **1989**, *62*(8), 929-932.
(14) Felter, T. E.; Hubbard, A. T. *J. Electroanal. Chem.* **1979**, *100*, 473-491.
(15) Wieckowski, A.; Schardt, B. C.; Rosasco, S. D.; Stickney, J. L.; Hubbard, A. T. *Surf. Sci.* **1984**, *146*, 115-134.
(16) Zurawski, D.; Rice, L.; Hourani, M.; Wieckowski, A. *J. Electroanal. Chem.* **1987**, *230*, 221-231.
(17) Schardt, B. C.; Yau, S.-L.; Rinaldi, F. *Science* **1989**, *243*, 1050-1053.

0002-7863/90/1512-3677$02.50/0

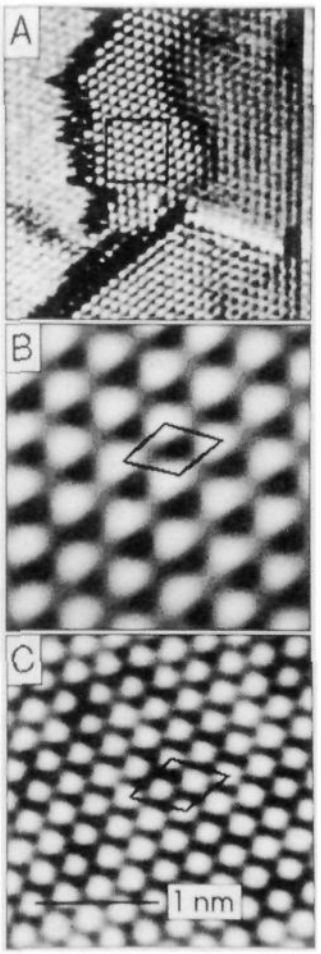

Figure 1. (A) In situ STM image of the Pt(111)-($\sqrt{3}\times\sqrt{3}$)R30°-I adlattice. Image was taken in 0.1 M $HClO_4$. Scan size = 12.5 nm, V_b = 31 mV, I_t = 25 nA. (B) Magnified image (2.5 nm) taken from the boxed region of image A. The rhombic ($\sqrt{3}\times\sqrt{3}$)R30° unit cell is outlined in black. (C) STM image (2.5 nm) of the Pt(111) substrate lattice showing the substrate orientation, V_b = 31 mV, I_t = 15 nA. A rhombic ($\sqrt{3}\times\sqrt{3}$)R30° unit cell is outlined in black for comparison to image B.

Ex situ UHV results suggest that the ($\sqrt{3}\times\sqrt{3}$)R30° structure is the predominate phase in electrolyte solution within a certain potential and pH range.[18,19] In situ STM while the surface is under potential control should allow direct observation of the low-coverage phase. In situ STM was performed by using a modified Nanoscope II[20] interfaced to a home-built bipotentiostat.[21] Insulated tungsten tunneling probe tips were used.[22] The Pt(111) surface was first annealed and dosed to ($\sqrt{7}\times\sqrt{7}$)-R19.1°-I. The surface was then mounted in the electrochemical cell of the modified STM, and 0.5 mL of 0.1 M $HClO_4$ was added to the cell. At the rest potential, we observed the expected ($\sqrt{7}\times\sqrt{7}$)R19.1°-I adlattice structure. The images obtained for the ($\sqrt{7}\times\sqrt{7}$)R19.1°-I structure in situ were identical with those obtained when imaging was carried out in air and so are not reproduced here. Upon lowering of the potential of the surface by 500 mV, the image shown in Figure 1A was obtained.[23] There is a monoatomic step running vertically through the left part of the image. To the right of the terrace edge is a region approximately 3.5 nm wide with a well-resolved atomic lattice. A 2.5-nm portion of this region, outlined by the black square in Figure 1A, was filtered and magnified to produce Figure 1B. Interpretation of the lattice image requires knowledge of the orientation of the substrate as mounted on the microscope. In earlier work, we utilized results from Laue back-reflection X-ray photography to roughly mount the surface in a preferred orientation. Since that time we have developed a simple means for reproducibly mounting the surface in a specific orientation.[24] The orientation of the surface can be taken from the Pt(111) substrate lattice image shown in Figure 1C. Figures 1B and 1C are the same magnification. An interactive computer graphics program was used to outline a rhombic ($\sqrt{3}\times\sqrt{3}$)R30° unit cell on the Pt(111) substrate image. The unit-cell outline was then duplicated and transferred onto the image shown in Figure 1B. The match of image 1B to ($\sqrt{3}\times\sqrt{3}$)R30° is quite good. The distortion evident in the unit cell was due to thermal drift, which tends to be more of a problem with in situ STM measurements as opposed to ex situ measurements. During several hundred hours imaging iodine dosed Pt surfaces in ambient air, we have never observed the ($\sqrt{3}\times\sqrt{3}$)R30° adlattice. The expected registry of the ($\sqrt{3}\times\sqrt{3}$)R30° lattice to the substrate would place all the iodine atoms at fcc 3-fold hollow sites on the Pt(111) surface. Experimental determination of the registry will require imaging of a domain boundary between the ($\sqrt{3}\times\sqrt{3}$)R30° lattice and the ($\sqrt{7}\times\sqrt{7}$)R19.1°-I adlattice which has a known registry with the substrate. This is one area in which we are continuing our investigations of this system.

We have also used in situ STM to study the molecular details of the nucleation and growth of Cu electrodeposits.[25] We expect that there will be many other interesting applications of this approach to the study of molecular phenomena at electrode surfaces.

An image of a platinum(111) substrate lattice was used to aid interpretation of the in situ images of the ($\sqrt{3}\times\sqrt{3}$)R30° adlattice. The origin of the image requires some explanation. In obtaining the substrate lattice image, a platinum(111) crystal was gas phase dosed with iodine as usual; however, the procedure for preparing the tunneling tips was modified. Our usual tip preparation procedure involves electrochemically etching a tungsten wire immersed in 1 M KOH solution. We attempted to improve the imaging resolution of the etched tips by following the electrochemical etch with a brief 15-s exposure of the top to a hot I_2/N_2 gas stream. Our experience with this modified procedure is limited; however, it has yielded tips with significantly different imaging properties from tips that were simply electrochemically etched. The STM images produced by the treated tip were very dependent upon choice of the tunneling bias voltage. At bias voltages from 200 mV down to 35 mV, the iodine adlattice was imaged. Below 35 mV, the platinum substrate lattice was imaged. Imaging the iodine adlattice or the substrate lattice was reversibly selectable by changing the bias voltage. Tungsten tips that are only electrochemically etched do not show this behavior and image the iodine adlattice over the bias potential range of 200 mV down

(18) Lu, F.; Salaita, G. N.; Baltruschat, H.; Hubbard, A. T. *J. Electroanal. Chem.* **1987**, *222*, 305–320.

(19) Mebrahtu, T.; Rodriguez, J. F.; Bravo, B. G.; Soriaga, M. P. *J. Electroanal. Chem.* **1987**, *219*, 327.

(20) The electrochemical cell was machined from a cylindrical ring of Kel-F. The open base of the electrochemical cell was sealed to the Pt(111) surface by a steel compression fitting screwed into the base of the microscope. The cell volume was 0.5 mL.

(21) The bipotentiostat was designed so that the potential of the tip and the surface could be independently controlled relative to a reference electrode. The power for the bipotentiostat was tapped from the Nanoscope II electronics. The control voltage for the surface potential was derived from a BAS CV-27 potentiostat through a high-precision instrumentation amplifier, Analog Devices 524AD. This scheme effectively eliminates the formation of ground loops and the resultant noise that can occur when a potentiostat is coupled to an STM.

(22) Immediately prior to use, a 0.010-in. tungsten wire was etched to a sharp point in 1 M KOH solution. After mounting in the tunneling head, the tip was painted with nail polish. The coating was allowed to dry for 10 min. No unusual steps were required for engaging the tip for tunneling.

(23) The data from the Nanoscope II was converted into an 8-bit tagged image file format (TIFF) and subsequently annotated by using a commercial Macintosh II computer graphics program. The image was then photographed from the Macintosh II video monitor using a 210-mm lens and a Canon EOS 620 camera.

(24) A 0.060-in.-wide mesa was machined into the back face of the platinum single crystal. A mating trough was machined into the stage of the microscope.

(25) Yau, S.-L.; Schardt, B. C., manuscript in preparation.

to 1 mV. Looking into these unusual properties in detail is clearly desirable; however, this has been impeded by our inability to routinely prepare tips with the properties just described.

Acknowledgment. This work was supported by the Industrial Associates program at Purdue University funded in part by Dow Chemical Co. and BP America.

Conformation–Reactivity Correlations in the Solid-State Photochemistry of Macrocyclic Diketones

Thillairaj Johnathan Lewis, Steven J. Rettig, John R. Scheffer,* James Trotter,* and Fred Wireko

Department of Chemistry
University of British Columbia
Vancouver, British Columbia, Canada V6T 1Y6

Received November 6, 1989

As part of a research program designed to investigate the crystalline-phase photochemistry of a wide variety of organic systems,[1] our interest in macrocyclic diketones was aroused by a paper reporting the crystal structure of the 18-membered-ring "diametric" diketone, cyclooctadecane-1,10-dione (**1b**, Scheme I).[2] This report indicated that **1b** has an intramolecular, six-membered cyclic C=O···H contact of 2.8 Å in the crystal that should allow for Norrish type II photoreaction[3] in this medium. Previous studies from our laboratory have shown that intramolecular hydrogen abstraction reactions in the solid state are feasible over C=O···H distances of approximately 3 Å or less.[4]

In the present communication, we report that diketone **1b** does in fact undergo Norrish type II photoreaction in the solid state. Two additional macrocyclic diketones were also investigated: the 16-membered analogue, cyclohexadecane-1,9-dione (**1a**), and the 22-membered compound, cyclodocosane-1,12-dione (**1c**);[5] each was analyzed crystallographically for the first time and photolyzed in the solid state. For comparison purposes, all three macrocyclic diketones were also irradiated in solution. Overall, the results provide valuable information on (1) the preferred conformations of the 16- and 22-membered-ring diametric diketones, (2) favorable six-membered transition state hydrogen atom abstraction distances, (3) the effect of molecular conformation on Norrish type II reactivity, and (4) novel crystal lattice medium effects in organic photochemistry.

The X-ray crystal structures of diketones **1a** and **1c**[6a] reveal that they too have close C=O···H_γ contacts that are favorable for type II photochemistry. Stereodiagrams showing the molecular conformations and closest C=O···H_γ contacts are given in Figure 1.[7] We note that diketone **1a** has the rectangular [3535] conformation predicted by Allinger, Gorden, and Profeta[8] and not the square [4444] structure predicted by Alvik, Borgen, and Dale.[9]

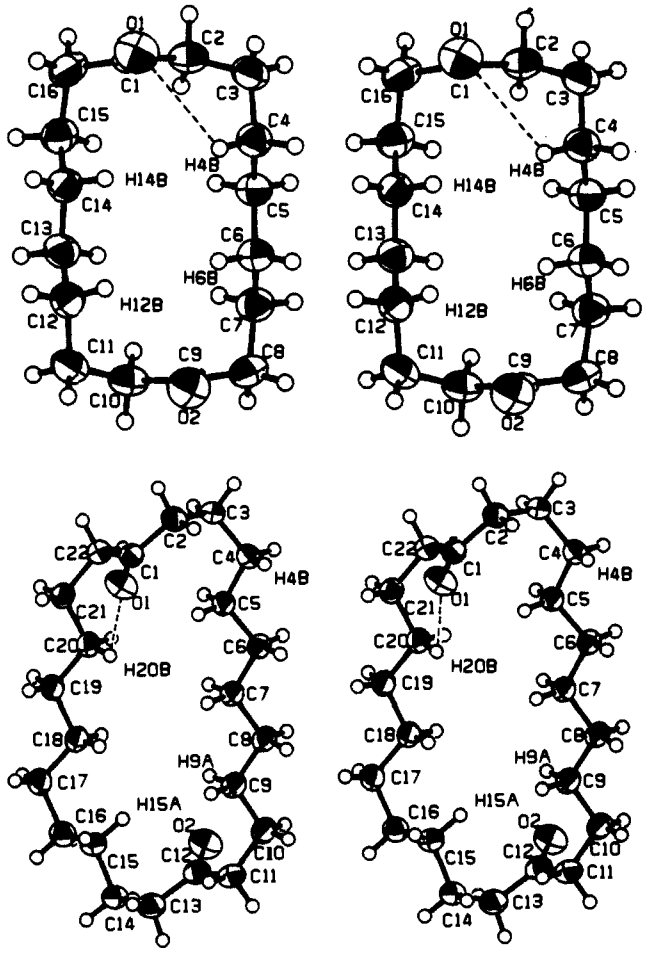

Figure 1. ORTEP stereodiagrams of diketones **1a** (top) and **1c** (bottom), showing 50% probability ellipsoids and atom labeling. The dotted lines indicate the shortest C=O···H_γ contacts (2.7 Å in each case).[7]

Scheme I

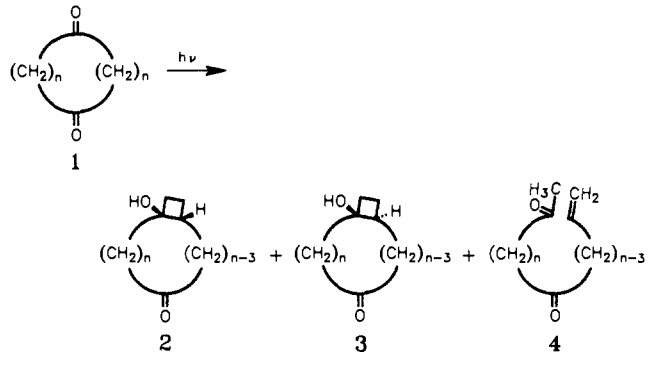

(a) n=7 (b) n=8 (c) n=10

As outlined in Scheme I, irradiation of diketones **1a–c** to low conversions, both in the solid state and in solution, led to three photoproduct types: the *cis*- and *trans*-cyclobutanols **2a–c** and **3a–c** (type II cyclization)[3] and the ene-diones **4a–c** (type II elimination).[3] Eight of the nine photoproducts were isolated and fully characterized. The ninth, cyclobutanol **2b**, could never be completely freed of its isomer, **3b**, and was therefore analyzed spectroscopically as a mixture. There was some ambiguity in assigning the cyclobutanol ring junction stereochemistry, but this was overcome by obtaining the crystal structure of cyclobutanol **2a**.[6b] With the configuration of **2a** (and, by default, that of **3a**) known with certainty, NMR correlations enabled the remaining stereochemical assignments to be made confidently.

(1) Scheffer, J. R.; Garcia-Garibay, M.; Nalamasu, O. In *Organic Photochemistry*; Padwa, A., Ed.; Marcel Dekker: New York, 1987; Vol. 8; pp 249–347.

(2) Allinger, N. L.; Gorden, B. J.; Newton, M. G.; Lauritsen-Norskov, L.; Profeta, S., Jr. *Tetrahedron* **1982**, *38*, 2905.

(3) Review: Wagner, P. J. In *Molecular Rearrangements in Ground and Excited States*; de Mayo, P., Ed.; Wiley-Interscience: New York, 1980; Chapter 20.

(4) Scheffer, J. R. In *Organic Solid Sate Chemistry*; Desiraju, G. R., Ed.; Elsevier: New York, 1987; Chapter 1.

(5) Compounds **1a–c** were prepared according to the procedure of Blomquist et al.: Blomquist, A. T.; Prager, J.; Wolinsky, J. *J. Am. Chem. Soc.* **1955**, *77*, 1804.

(6) (a) Diketone **1a**: $P\bar{1}$; a = 9.866 (1) Å, b = 14.923 (2) Å, c = 5.453 (1) Å; α = 95.03 (2)°, β = 90.42 (2)°, γ = 75.38 (1)°; Z = 2; R = 3.6%. Diketone **1c**: $P2_1/c$; a = 15.408 (1) Å, b = 5.508 (1) Å, c = 24.696 (1) Å; β = 99.662 (5)°; Z = 4; R = 4.7%. (b) Cyclobutanol **2a**: $P\bar{1}$; a = 9.784 (2) Å, b = 9.885 (3) Å, c = 9.580 (3) Å; α = 116.59 (2)°, β = 109.88 (2)°, γ = 95.91 (2)°; Z = 2; R = 3.8%.

(7) Only the closest C=O···H_γ contacts are given. In the case of **1a**, abstraction of H14B (2.9 Å), H12B (2.8 Å), or H6B (2.9 Å) is also possible (<3 Å). For **1c**, abstraction of H9A (2.8 Å) is also feasible.

(8) Allinger, N. L.; Gorden, B.; Profeta, S., Jr. *Tetrahedron* **1980**, *36*, 859.

(9) Alvik, T.; Borgen, G.; Dale, J. *Acta Chem. Scand.* **1972**, *26*, 1805.

0002-7863/90/1512-3679$02.50/0